Spin transport in benzofurane bithiophene based organic spin valves

Mathieu Palosse, Isabelle Séguy, Eléna Bedel-Pereira, Christina Villeneuve-Faure, Charlotte Mallet, Pierre Frère, Bénédicte Warot-Fonrose, Nicolas Biziere, Jean-François Bobo

Spin transport in benzofurane bithiophene based organic spin valves

Cite as: AIP Advances **4**, 017117 (2014); https://doi.org/10.1063/1.4862675
Submitted: 19 July 2013 . Accepted: 06 January 2014 . Published Online: 15 January 2014

Mathieu Palosse, Isabelle Séguy, Élena Bedel-Pereira, Christina Villeneuve-Faure, Charlotte Mallet, Pierre Frère, Bénédicte Warot-Fonrose, Nicolas Biziere, and Jean-François Bobo

Spin transport in benzofurane bithiophene based organic spin valves

Mathieu Palosse,[1,2] Isabelle Séguy,[1,2] Élena Bedel-Pereira,[1,2]
Christina Villeneuve-Faure,[2,3] Charlotte Mallet,[4] Pierre Frère,[4]
Bénédicte Warot-Fonrose,[2,5] Nicolas Biziere,[2,5] and Jean-François Bobo[2,6,a]

[1]*CNRS, LAAS, 7 avenue du Colonel Roche, F-31400 Toulouse, France*
[2]*Université de Toulouse; UPS, INSA, INP, ISAE; LAAS; CEMES, F-31077 Toulouse France*
[3]*LAPLACE, Université Paul Sabatier, 118, route de Narbonne 31062 Toulouse Cedex 9 France*
[4]*MOLTECH-Anjou, UMR CNRS 6200, Université d'Angers, 2 Bd Lavoisier 49045 ANGERS Cedex France*
[5]*CNRS, CEMES-CNRS UPR 8011, 29 rue Jeanne Marvig, BP 94347, FR-31055 Toulouse Cedex 4 France*
[6]*CNRS, CEMES-ONERA, NMH, 2 avenue Edouard Belin, FR-31055 Toulouse Cedex 4 France*

(Received 19 July 2013; accepted 6 January 2014; published online 15 January 2014)

In this paper we present spin transport in organic spin-valves using benzofurane bithiophene (BF3) as spacer layer between NiFe and Co ferromagnetic electrodes. The use of an AlO_x buffer layer between the top electrode and the organic layer is discussed in terms of improvements of stacking topology, electrical transport and oxygen contamination of the BF3 layer. A study of magnetic hysteresis cycles evidences spin-valve behaviour. Transport properties are indicative of unshorted devices with non-linear *I-V* characteristics. Finally we report a magnetoresistance of 3% at 40 K and 10 mV in a sample with a 50 nm thick spacer layer, using an AlO_x buffer layer. [http://dx.doi.org/10.1063/1.4862675]

Organic semiconductors (OSC) have drawn increasing interest in spintronics since the first evidence of magnetoresistance in sexithiophene (6T)[1] and tris(8-hydroxyquinoline) aluminum (Alq_3)[2] based spin-valves. The choice of an organic semiconductor instead of an inorganic one is driven by the amount of interesting properties OSCs feature: potentially long spin relaxation time,[3] chemical tuning of electronic functionality, easy structural modification, possibility of self-assembly and mechanical flexibility. Though magnetoresistance (MR) seems to be obtained in most organic spin-valves (OSV), injection and transport of spin polarized current in OSC, and the role played by the interfaces between the organic layer and the ferromagnetic (FM) electrodes are still matters of discussion.[4,5]

As reviewed recently,[6] most organic spintronics devices are based on Alq_3[7–10] as transport layer for spin-polarized charge carrier although many other π-conjugated systems have been synthesized by chemists. Among the results obtained with Alq_3, a large dispersion of MR values, from -300% to +8%, has to be explained.[2,8,9,11]

Alq_3 is well known as an electron transport OSC with low electron mobility, about $10^{-6}\ cm^2V^{-1}s^{-1}$ and also lower hole mobility[12] of $10^{-8}\ cm^2V^{-1}s^{-1}$. Moreover, the energy gap between the Alq_3 lowest unoccupied molecular orbital (LUMO) and the FMs electrodes Fermi

[a]Author to whom correspondence should be addressed. Electronic adress: jfbobo@cemes.fr

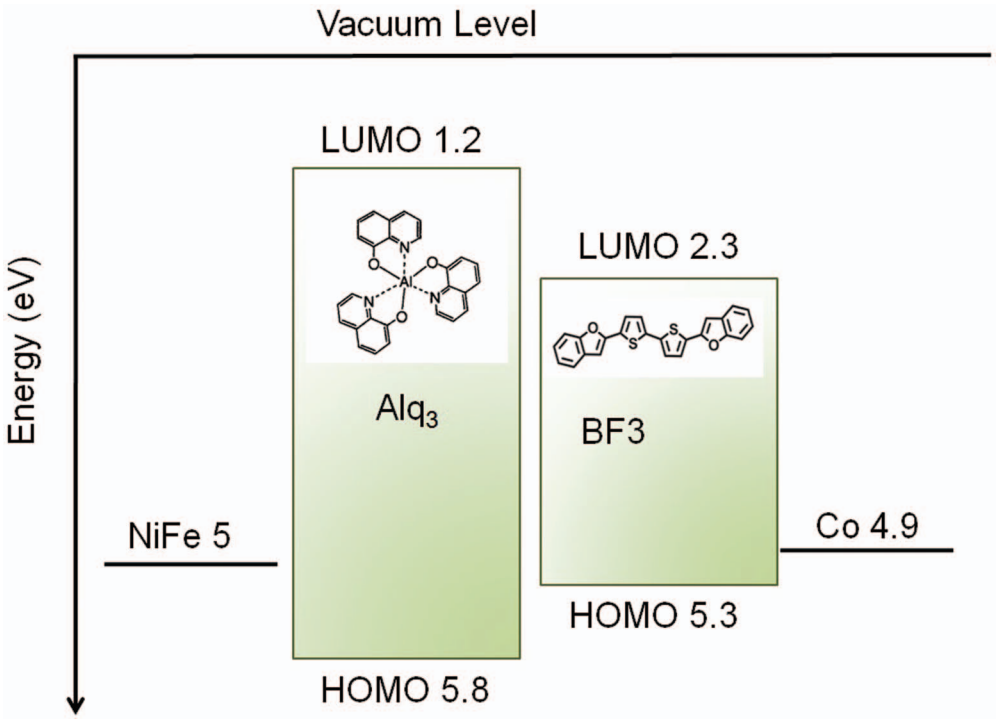

FIG. 1. Schematic energy level diagram showing the Alq_3 and BF3 molecular levels and workfunctions of the FM electrodes (inset: molecular structure of Alq_3 and BF3).

levels can involve an important energy injection barrier for electrons (Fig. 1(a)). In this figure, the displayed experimental highest occupied molecular orbital (HOMO) and LUMO values for Alq_3 were determined by Hill *et al.*[13] by ultraviolet phoelectron spectroscopy (UPS) and inverse photo-electron spectroscopy (IPES) and give transport gap larger than the usually encountered optical gap obtained by absorption measurements. Although it has been pointed out that interface dipoles lower the potential barrier height of the Alq_3-FM electrodes junction,[14] the question of holes instead of electrons injection and transport in Alq_3 based OSVs has been raised.[15]

In this paper we present investigations of OSV based on benzofurane bithiophene (BF3) sandwiched between NiFe and Co electrodes. The chemical structure of BF3 is shown in inset of figure 1. BF3 is an ideal choice, among OSCs since it exhibits high hole mobility in air at room temperature,[16] up to 9.3 $10^{-3} cm^2 V^{-1} s^{-1}$, and good thermal stability with a decomposition temperature of 293 °C. The HOMO and LUMO energy levels have been calculated by DFT methods and are found to be 5.3 eV and 2.3 eV respectively[16] (UPS and IPES data not available for BF3 at present time). This result shows that BF3 HOMO matches quite well with energy Fermi levels of the electrodes chosen here (Fig. 1).

The devices typical structure consists of glass/NiFe/BF3(/AlO_x)/Co, patterned for a current perpendicular to plane (CPP) geometry with or without optional AlO_x buffer. The upper Co and bottom NiFe FM electrodes are prepared by dc sputtering with 5×10^{-3} mB Ar pressure through appropriate contact masks, resulting in devices with junction areas of $200 \times 200\ \mu m^2$. BF3 films are grown by Joule evaporation in a high vacuum (10^{-7} mB) chamber connected to the sputter chamber. Masks are changed in situ using a micromanipulator and a homemade sample holder, preventing the sample from atmospheric exposure during mask changing. As direct Co sputtering is harmful for the organic layer, we add a 2 nm thick AlO_x protective buffer layer between the upper electrode and the organic film, to prevent Co atoms to penetrate into the organic film.[8,10,17] Note that this aluminum oxide layer is not insulating enough for blocking carrier injection in the OSC.

This oxide buffer layer is obtained by O_2 exposure (30 mB) of two consecutive 1 nm sputtered Al films. Sample topological properties are studied on each successively grown layer by atomic

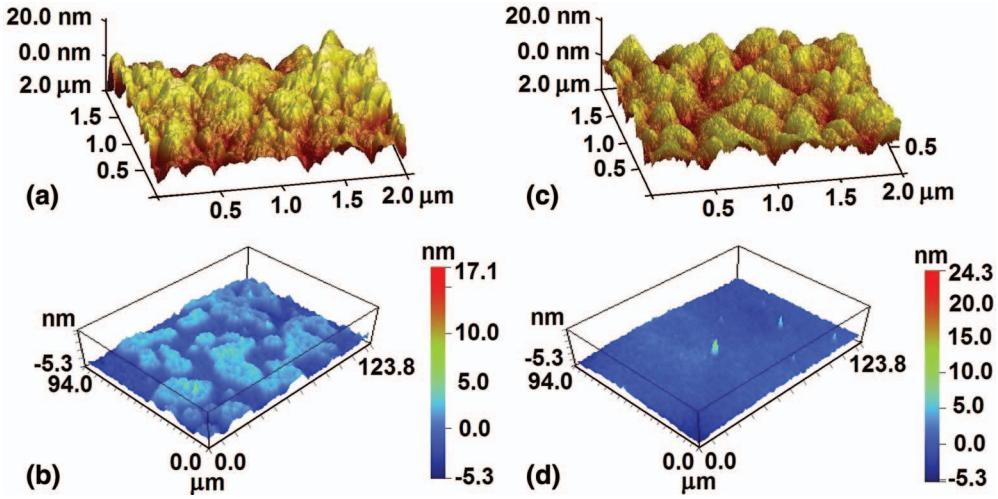

FIG. 2. Morphological properties of a NiFe/BF3 (50 nm)/Co sample: a) & b) without AlO_x; c) & d) with AlO_x; by a) & c) AFM tapping mode, scan size 2 × 2 μm^2 and b) & d)Optical profilometer, scan size 124 × 94 μm^2.

force microscopy (AFM) using a Dimension 3100 Nanoscope AFM in tapping mode. For a more representative area investigation of our samples junctions, complementary study is required with Veeco optical profilometer (124 × 94 μm^2). Magnetic properties are investigated with a commercial Quantum Design Physical Properties Measurement System (PPMS) with a VSM module (Vibrating Sample Magnetometer). Transport and magnetotransport measurements are performed using a Keithley 2400 sourcemeter in 2 probes mode connected to the PPMS for temperature control, from 300 to 5 K. Magnetic field is applied within ± 10 kOe range in the plane of the substrate.

First, AFM and optical profilometer studies are done on samples from the same batch of NiFe/BF3 (50 nm) with or without an AlO_x barrier (Fig. 2) for comparison. They reveal a low roughness of the bottom NiFe electrode (rms=1 nm). The observed organic layer rms roughness is 5 nm for both samples, with or without an AlO_x barrier. In samples including AlO_x, this buffer layer grows conformal to the OSC, and non significant roughness changes are observed after Co deposition. Roughness is more important in samples without an AlO_x barrier, and a blistered surface evidences the damage caused to the organic layer during Co sputtering (see Fig. 2(b)). All samples without an AlO_x barrier are also found to be electrically shorted. These results are proofs that the AlO_x barrier we added provides an efficient protection for the organic layer. The achievement of smooth morphological properties allows to investigate magnetic properties of full plane stacking on Si substrates.

VSM measurements between ± 1 kOe reveal uncoupled magnetic electrodes, a critical property for achieving spin valve behaviour and magnetotransport (Fig. 3). The influence of temperature on the switching fields of the Co layer is also to be noted. We observe an increase from 20 Oe and - 20 Oe at 300 K to 200 Oe and -750 Oe at 10 K. The asymmetrical dependence of the increase of the switching field when temperature decreases can be explained by the formation of a CoO_x antiferromagnetic layer on top of the Co layer due to air exposure of the top layer of the device after sample preparation. This leads to exchange coupling between ferromagnetic Co and antiferromagnetic CoO_x of the hysteresis cycle of the Co layer after a positive field cooling. Nevertheless, this phenomenon does not constitute a spin valve behaviour issue.

Transport measurements between ± 10 V show non-linear *I-V* characteristics that obey a power law (inset Fig. 4). Data analysis allows us to exclude injection-limited device operation in favour of a mechanism governed by transport. Temperature dependence is also to be noted: the hybrid junction resistance displays a ten-fold increase between room temperature and 10 K, indicative of a semiconductor behaviour, and excluding tunnel MR in our samples.[18] Temperature dependence of the resistance between 10 and 40 K follows a Mott's type Various Range Hopping (VRH) model[19] (see Fig. 5), in which $R(T)=R_0 \exp(T_0/T)^{1/4}$. This is characteristic of multistep tunnelling through

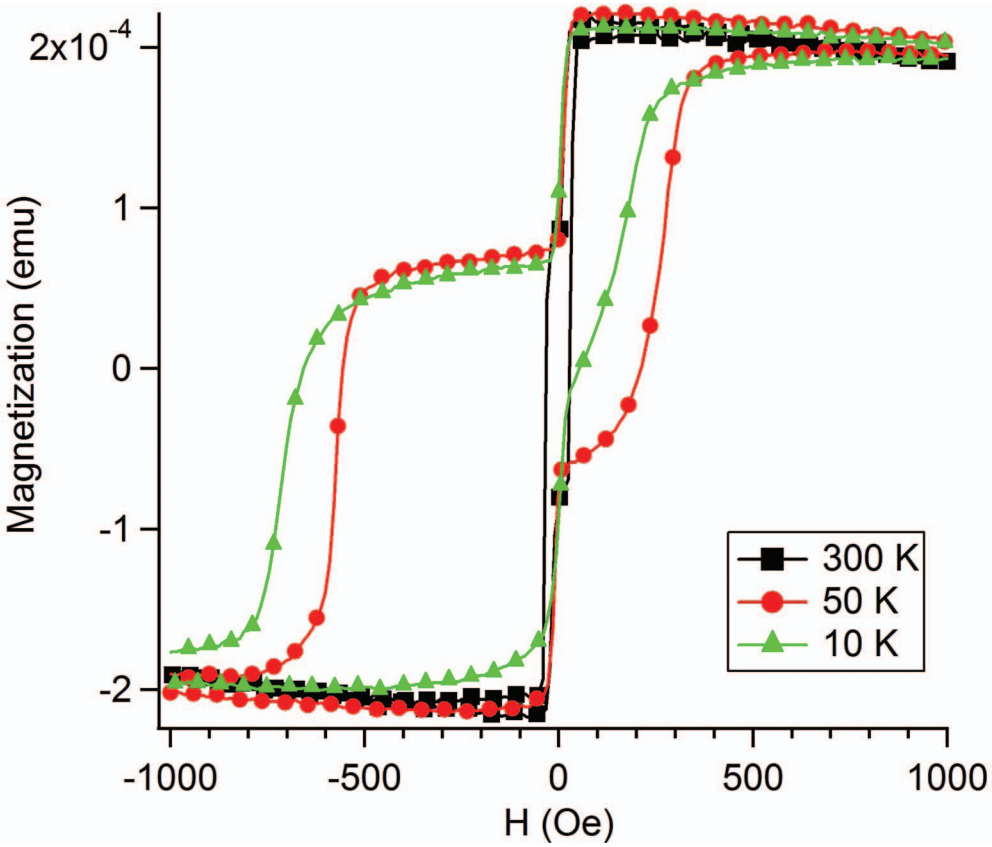

FIG. 3. VSM measurements at different temperatures of a NiFe/BF3 (50 nm)/AlO_x/Co sample.

the organic layer.[20] Further experiments are in progress to analyze temperature dependence of the resistance at higher temperatures. Magnetotransport is then studied on a sample of glass/NiFe/BF3 (50 nm)/AlO_x/Co, in the range of $\pm$ 5 kOe, applying bias voltage from 70 mV to - 70 mV. It reveals a MR of 2–3 % at 40 K using a bias voltage of 10 mV on the Co top electrode (Fig. 4). For T larger than 40 K MR is not detected in our sample. We attribute that to the existence of other transport mechanisms based on hoping that increase spin relaxation and induce a loss of spin-polarized transport in our sample. At lower temperature, our device became too resistive (R $>$ 20 MOhm) and signal was too noisy for proper MR measurement. A MR decrease is noted when increasing voltage and MR gets down to low values at 70 mV (Fig. 4). This behaviour is symmetrical, applying bias voltage either on the NiFe or Co electrode. Our VRH modeling of R(T) characteristics show a neat voltage dependence of the transport mechanism. This is indicative of the creation of new current channels in the BF3 layer with multistep tunneling that will have an effect on the loss of spin polarization of the current and consequently on the observed voltage decay of the MR. We also observe $\approx$ 1 % MR for another sample with 110 nm BF3 layer.

We notice that all samples display poor time stability. This phenomenon can be attributed to the oxidative degradation of the OSC during the fabrication of the AlO_x barrier. In order to clarify this point, low temperature photoluminescence (low-T PL) experiments are performed on pristine BF3 films with and without oxygen exposure (two steps 25 min controlled oxidation, at room temperature and O_2 pressure = 30 mB, similar to AlO_x buffer layer preparation). Indeed, it has been shown that low-T PL is very sensitive to OSC oxidation damage.[21] PL is excited by a 40 mW laser diode at λ_{ex} = 405 nm (peak of BF3 absorption). Spectra were analyzed by a 1 m focal length grating monochromator and detected by a R636 Hamamatsu photomultiplier and standard lock-in techniques. The sample was cooled at 12 K using a closed cycle He cryostat. As shown in Fig. 6, slight peak shift (under 0,05 eV) suggests OSC layers inhomogeneities, but no effect of

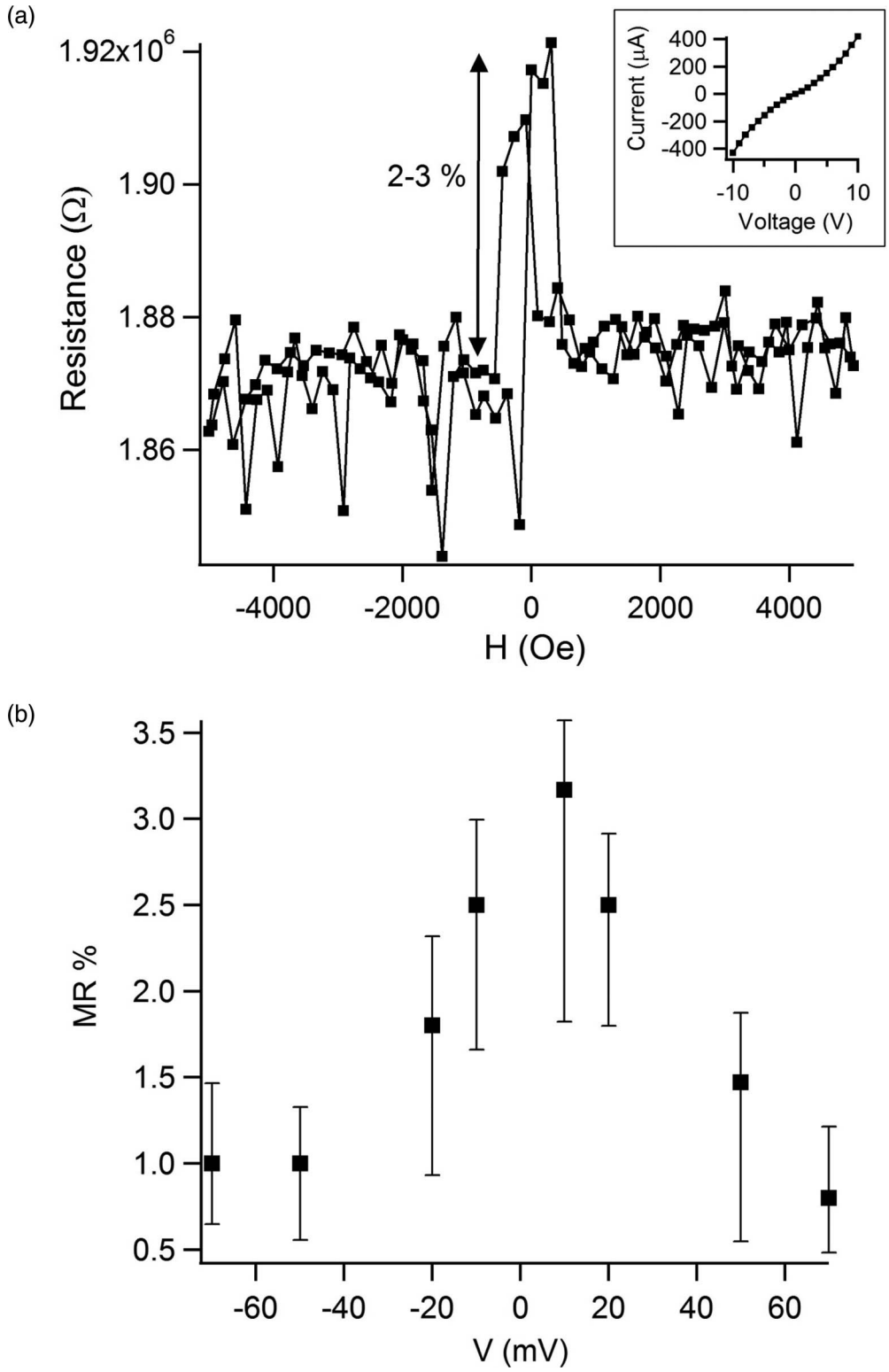

FIG. 4. a) Resistance versus magnetic field for a NiFe/BF3 (50 nm)/AlO_x/Co sample at 40 K and 10 mV (Co anode). Inset : non linear *I-V* curve for the same sample. b) MR versus bias voltage with error bars for a NiFe/BF3 (50 nm)/AlO_x/Co sample at 40 K (Co anode).

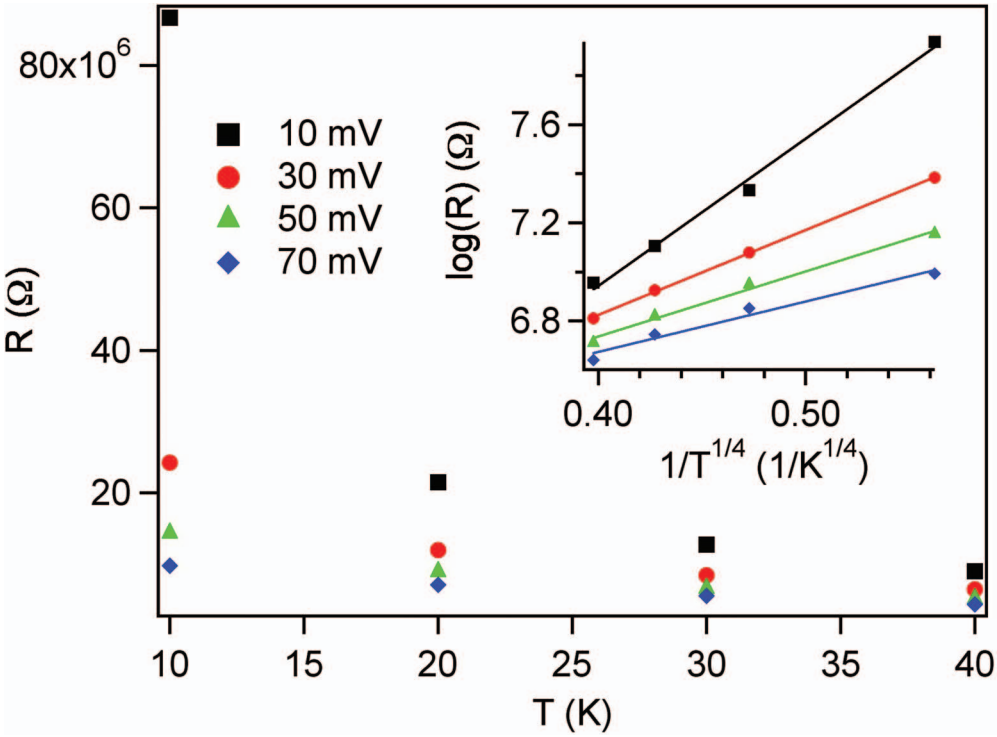

FIG. 5. Resistance versus temperature data for a NiFe/BF3 (50 nm)/AlO_x/Co sample and various applied voltages (Co anode). Inset : VRH fittings of these data (see text).

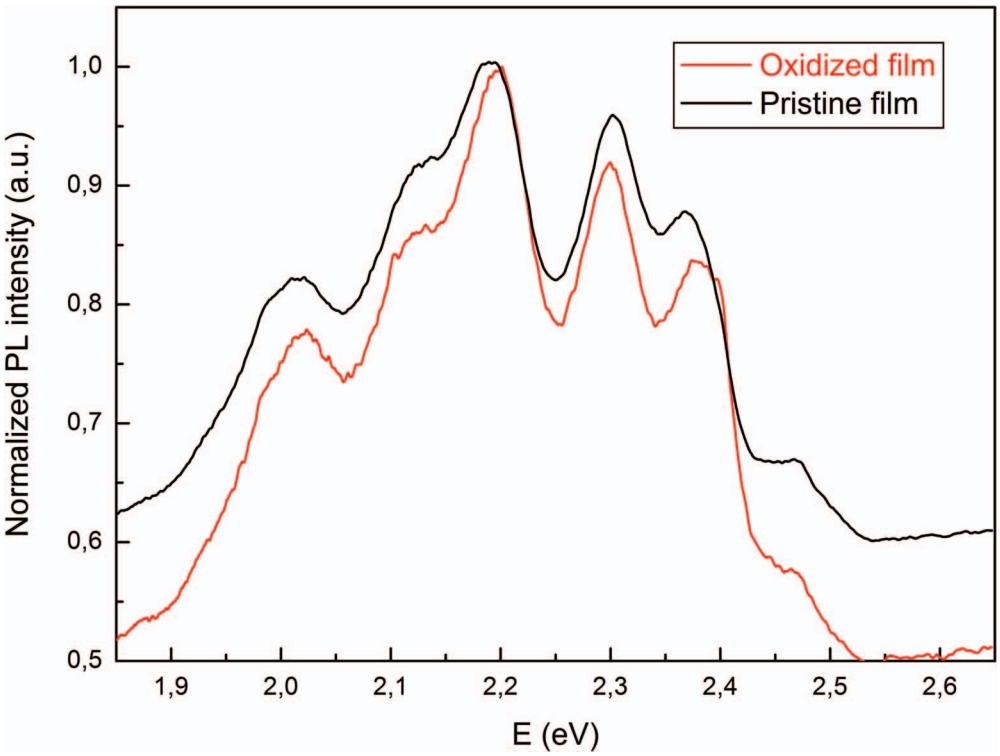

FIG. 6. Low temperature photoluminescence spectra of a pristine and an oxidized BF3 film.

O_2 exposure is observed on PL spectra. This is evidence of no oxidative defects formation in BF3 thin films. Consequently, we assume that, either thin Al layer provides efficient protection against oxidation, or the BF3 molecules are very stable when exposed to O_2 (as air mobility measurements tend to show[16]). So we conclude that our devices time instability is not due to oxygen contamination of BF3 but rather to OSC layer inhomogeneities or metallic contamination from FM electrodes. STEM-EELS (Scanning Transmission Electron Microscopy-Electron Energy Loss Spectroscopy) experiments are in progress in order to confirm this issue.

In summary, we have prepared organic spin valves with BF3 spacer layer and we observed up to 3% MR in samples with 50 nm BF3 thickness topped with 2 nm AlO_x. In this case, aluminium oxide layer is an efficient protection of BF3 prior to the deposition of the top cobalt film of the structure. Our results demonstrate the stability of BF3 to oxygen, its ability as a spin transport material with a relatively large spin diffusion length since we observed MR up to 110 nm organic layer.

This work was partly supported by the French RENATECH network.

[1] V. Dediu, M. Murgia, F. C. Matacotta, C. Taliani, and S. Barbanera, Solid State Commun. **122**, 181 (2002).
[2] Z. H. Xiong, D. Wu, Z. V. Vardeny, and J. Shi, Nature **427**, 821 (2004).
[3] S. Sanvito and A. R. Rocha, J. Comput. Theor. Nanos. **3**, 624 (2006).
[4] G. Szulczewski, S. Sanvito, and M. Coey, Nat. Mater. **8**, 693 (2009).
[5] C. Barraud, P. Seneor, R. Mattana, S. Fusil, K. Bouzehouane, C. Deranlot, P. Graziosi, L. Hueso, I. Bergenti, V. Dediu, F. Petroff, and A. Fert, Nat. Phys. **6**, 615 (2010).
[6] V. A. Dediu, L. E. Hueso, I. Bergenti, and C. Taliani, Nat. Mater. **8**, 707 (2009).
[7] F. J. Wang, Z. H. Xiong, D. Wu, J. Shi, and Z. V. Vardeny, Synth. Met. **155**, 172 (2005).
[8] V. Dediu, L. E. Hueso, I. Bergenti, A. Riminucci, F. Borgatti, P. Graziosi, C. Newby, F. Casoli, M. P. De Jong, C. Taliani, and Y. Zhan, Phys. Rev. B **78**, 115203 (2008).
[9] Y. Liu, S. M. Watson, T. Lee, J. M. Gorham, H. E. Katz, J. A. Borchers, H. D. Fairbrother, and D. H. Reich, Phys. Rev. B **79**, 075312 (2009).
[10] T. S. Santos, J. S. Lee, P. Migdal, I. C. Lekshmi, B. Satpati, and J. S. Moodera, Phys. Rev. Lett. **98**, 016601 (2007).
[11] D. Sun, L. Yin, C. Sun, H. Guo, Z. Gai, X.-G Zhang, T. Z. Ward, Z. Cheng, and J. Shen, Phys. Rev. Lett. **104**, 236602 (2010).
[12] R. G. Kepler, P. M. Beeson, S. J. Jacobs, R. A. Anderson, M. B. Sinclair, V. S. Valencia, and P. A. Cahill, Appl. Phys. Lett. **66**, 3618 (1995).
[13] I. G. Hill, A. Kahn, Z. G. Soos, and R. A. Pascal, Jr., Chem. Phys. Lett. **327**, 181 (2000).
[14] M. A. Baldo and S. R. Forrest, Phys. Rev. B **64**, 085201 (2001).
[15] J. S. Jiang, J. E. Pearson, and S. D. Bader, Phys. Rev. B **77**, 035303 (2008).
[16] C. Mallet, Y. Didane, T. Watanabe, N. Yoshimoto, M. Allain, C. Videlot-Ackermann, and P. Frère, ChemPlusChem **78**, 459 (2013).
[17] Y. Q. Zhan, X. J. Liu, E. Carlegrim, F. H. Li, I. Bergenti, P. Graziosi, V. Dediu, and M. Fahlman, Appl. Phys. Lett. **94**, 053301 (2009).
[18] M. Grünewald, M. Wahler, F. Schumann, M. Michelfeit, C. Gould, R. Schmidt, F. Würthner, G. Schmidt, and L. W. Molenkamp, Phys. Rev. B **84**, 125208 (2011).
[19] N. F. Mott, J. Non-Cryst. Solids **1**, 1 (1968).
[20] S. Majumdar and H. S. Majumdar, Org. Elec. **13**, 2653 (2012).
[21] C. Carach and M. J. Gordon, J. Phys. Chem. B **117**, 1950 (2013).